Science of the Total Environment 701 (2020) 134648

Contents lists available at ScienceDirect

Science of the Total Environment

journal homepage: www.elsevier.com/locate/scitotenv

Molecular responses of an estuarine oyster to multiple metal contamination in Southern China revealed by RNA-seq

Yunlong Li [a], Xinhui Zhang [b], Jie Meng [c], Jieming Chen [b], Xinxin You [b], Qiong Shi [b], Wen-Xiong Wang [a,*]

[a] Department of Ocean Science and Hong Kong Branch of the Southern Marine Science and Engineering Guangdong Laboratory (Guangzhou), The Hong Kong University of Science and Technology (HKUST), Clear Water Bay, Kowloon, Hong Kong, China
[b] Shenzhen Key Lab of Marine Genomics, Guangdong Provincial Key Lab of Molecular Breeding in Marine Economic Animals, BGI Academy of Marine Sciences, BGI Marine, BGI, Shenzhen 518083, China
[c] Key Laboratory of Experimental Marine Biology, Institute of Oceanology, Chinese Academy of Sciences, Qingdao 266071, Shandong, China

HIGHLIGHTS

- Phenotypic differentiation of oysters under chronically metal exposure in the field.
- Gene expression patterns displayed differentiation among the three populations.
- Increasing expressions of Zn/Cu transporters and metallothionein explained their high accumulation.
- Energy production and cytoskeleton metabolism related genes were enriched in the contaminated sites.
- Oysters with less metal accumulation tended to cope with metal stress actively.

GRAPHICAL ABSTRACT

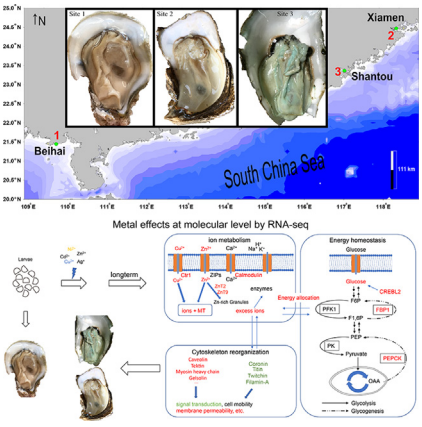

ARTICLE INFO

Article history:
Received 10 July 2019
Received in revised form 5 September 2019
Accepted 23 September 2019
Available online 24 October 2019

Editor: Daniel Wunderlin

Keywords:
Oysters
Metal contamination
Field population
Estuary

ABSTRACT

The estuarine oysters *Crassostrea hongkongensis* hyper-accumulate many metals and survive under high levels of metal exposure. In the present study, three natural populations of oysters with various levels of accumulated metals (mainly Cu and Zn) were collected from Southern China. The morphological characteristics and metal concentrations revealed their phenotypic differentiation. Further transcripts sequences acquired from their gill tissues were analyzed and 44,801 genes (with effective reads) were obtained via *de novo* assembly. The principal component analysis (PCA) revealed that the gene expression patterns also displayed differentiation among the three populations. A total of 3,199 differentially expressed genes (DEGs) was identified in the contaminated oysters as compared to the 'clean' oysters, which were used to explain the molecular mechanisms of metal accumulation and toxicity. GO and KEGG enrichment analysis revealed that energy production and cytoskeleton metabolism-related genes were particularly enriched in the contaminated sites during chronic metal exposure. Besides, increasing expressions of Zn/Cu transporters and metallothionein may explain their high accumulation in contaminated populations. We showed that oysters with less metal accumulation tended to cope with metal stress actively, but severe contamination destroyed part of the normal function. Our study analyzed the gene expression patterns of *C. hongkongensis* in Southern China and demonstrated the phenotypic differentiation of oysters under chronical metal exposure in the field.

* Corresponding author.
E-mail address: wwang@ust.hk (W.-X. Wang).

https://doi.org/10.1016/j.scitotenv.2019.134648
0048-9697/

1. Introduction

With rapid development of economy in China over the past few decades, industrial wastewaters containing high concentrations of trace metals were frequently released into the water environments, resulting in severe metal contamination in estuarine and coastal environments (Pan and Wang, 2012b). Organisms living in such environments are potentially under metal stress, leading to some abnormal phenomenon (e.g., colored oysters). Due to the capability of metal hyper-accumulation (e.g., up to 1.9% Cu and 2.4% Zn in dry weight of the total soft tissue, Wang et al., 2011) and their sessile habit, oysters *Crassostrea hongkongensis* are an ideal biomonitor/bioindicator of estuarine metal contamination. It is thus important to understand the various mechanisms employed by oysters to survive under such highly contaminated environments.

Oysters *C. hongkongensis* are mainly distributed in the estuarine areas of southern China, which contained multiple metal contaminants, and thus provide excellent subjects for ecotoxicological research (Lu et al., 2017; Wang et al., 2018). After the first discovery of blue-colored oyster *C. hongkongensis* in the Jiulong River Estuary in 2010 (Wang et al., 2011), abnormal oysters were also documented in other estuarine environments including the Pearl River Estuary and the Rong River Estuary (Liu et al., 2013). The blue colors indicated the hyperaccumulation of Cu and Zn. High concentrations of metals resulted in the differentiation of oysters, which could be easily distinguished from the uncontaminated ones.

Diverse tools have been applied to investigate the differentiation between metal-contaminated oysters and 'clean' ones. Subcellular measurements suggested that oysters sequestered metals in detoxified forms, which might explain why *C. hongkongensis* survived while accumulating such high metal concentration (Wang et al., 2011; Pan and Wang, 2012a). Under metal contamination, cellular debris was the main pool for Cu in *C. hongkongensis*, whereas metallothionein-like protein (MTLP) could bind with the increasing Zn (Yu et al., 2013). Also, biomarker measurements showed the possible MT contribution to the survival of oysters under high metal stress environments (Liu and Wang, 2016b). X-ray absorption spectroscopy revealed a higher proportion of metal-oxygen binding in colored oysters from Jiulong River Estuary contaminated by metals (Tan et al., 2015). However, subcellular distribution and speciation did not provide enough and accurate information to further explain the toxicity and process of metals in the blue-colored oyster at the molecular levels.

Due to the sensitive detection and high throughput, transcriptomics could investigate the profiles of messenger RNA (mRNA), providing more information on the toxicological responses (Heijne et al., 2005; Lacave et al., 2018; Liu et al., 2017; Qiao et al., 2018; Zhang et al., 2019). In the Pacific oyster *C. gigas* and the Pearl oyster *Princtada margaritifera*, transcriptome helped to reveal the molecular responses to metals (Pb, Cd, and Cr) and organic pollutants (e.g., herbicide diuron), including damage of DNA repair capacity, protein processing and oxidative stress (Bachère et al., 2017; Gueguen et al., 2017; Meng et al., 2017, 2018; Rondon et al., 2016). For example, transcriptomics identified the GABA transporter 2 gene (a neurotransmitter transporter, GAT2) as a key regulator in the hyper-accumulation of Cu in the oyster *C. angulata* (Shi et al., 2015). Also, relationship between DNA level and metal stress was investigated by whole genome re-sequencing, and genome variation (SNPs) was related to metal pollution in the Portuguese oyster *Crassostrea angulata* (Cross et al., 2014). However, the aforementioned transcriptomic studies relied on the laboratory exposed animals, whereas very few studies examined the natural populations of oysters differentially exposed to metals. Indeed, exposure experiment could limit the variables such that a single exposure could be carefully controlled, but such experiments can hardly mimic those occurring in the real environments.

In this study, oysters *C. hongkongensis* were sampled from three sites across southern China, including one relatively clean site and two contaminated sites. These oysters were then subjected to metal concentration measurements (Ag, Cd, Cr, Cu, Ni, Pb, and Zn) and RNA-sequencing (RNA-seq). With the different levels of metal accumulation, we attempted to identify the potential relationships with the molecular responses at the mRNA level provided by RNA-seq. This study contributed to the better understanding of mechanisms why oysters could accumulate high levels of trace metals and then survive in the polluted estuaries.

2. Materials and methods

2.1. Oysters sampling

In this study, we took the advantages of a wide range of metal contamination across the entire Southern China coastal environment, where *C. hongkongensis* inhabited. We collected oysters from three different sites where metal contaminants were of predominant concern (Fig. 1), especially for Cu and Zn. Site 1 was in Beihai (21°26′N, 109°18′E) in Guangxi Province, China, and remote from any metal pollution and thus regarded as the uncontaminated site. Site 2 was in the Jiulong River Estuary (24°28′N, 117°54′E) where Cu and Zn contaminations were observed. Site 3, situated in the Rong River Estuary in Shantou (23°22′N, 116°34′E), was the most severely contaminated one among the three sites and contained the highest metal concentrations. Samplings were completed within 7 days (August 28–September 3) in 2017.

At each site, 12 individual oysters with similar growing age (about 2 years, 8–10 cm shell length) were dissected immediately in the field. After rinsed by Milli-Q water, gill was selected carefully and divided into several pieces. All the samples were frozen in liquid nitrogen immediately. Samples for sequencing were stored at −80 °C, whereas the rest samples for metal concentration measurements were stored at −20 °C until further analysis.

2.2. Metal analysis

About 100 mg of the freeze-dried gills were digested with 3 ml 65% purified nitric acid (Sigma-Aldrich) for 12 h until completely digested at room temperature and 80 °C. Milli-Q (ultrapure) water and 65% nitric acid were used to dilute the acid solution to the appropriate range for measurements with a final 2.0% acid concentration. Inductively coupled plasma mass spectrometry (ICP-MS, NexION 300X, PerkinElmer) was used to measure the concentrations of metals (Ag, Cd, Cr, Ni, Pb, Cu, and Zn). Meanwhile, standard reference material (SRM 1566b, Sigma-Aldrich) certified by the National Institute of Standards and Technology was employed for method verification. The multi-element standards with 100 μg/ml mixed metals (Quality Control Standard 21, PerkinElmer) were also implemented as quality control (QC) in the analytical run. The diluted solution with 2 μg/L was measured every 10 oyster samples during the ICP-MS detection. In this study, the recoveries from standard reference materials were within 90–120%, and the values of QC were within 90–110%, indicating the reliable results. All values of metal concentrations were based on the dry weight of gill tissue.

2.3. RNA extraction and sequencing

In our study, a total of 12 replicated oyster individuals were collected from each site and their gills were used to measure the metal concentrations. Meanwhile, 5 individuals from each site

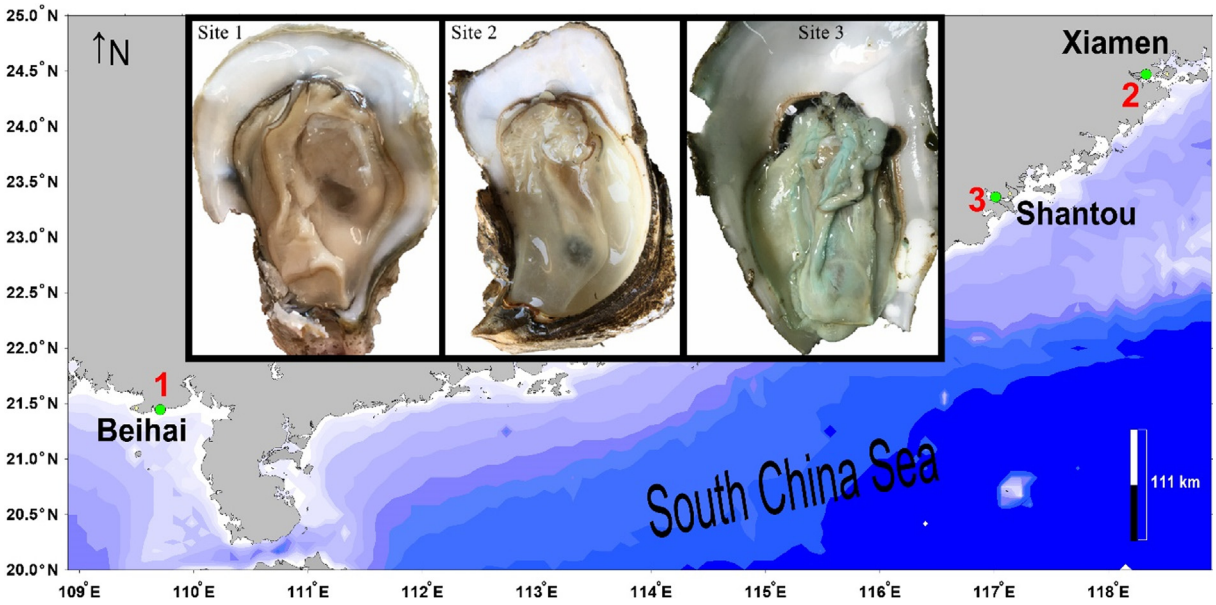

Fig. 1. Location of three sampling sites and the appearance of oysters. Normal oysters from Site 1 (Beihai, Guangxi Province), scrawny oysters with high water content from Site 2 (Jiulong River Estuary near Xiamen, Fujian Province), and blue-colored oysters from Site 3 (Rong River Estuary in Shantou, Guangdong Province). The map data was obtained from public information and graph was created by Surfer software. (For interpretation of the references to color in this figure legend, the reader is referred to the web version of this article.)

(i.e., 5 biological replicates from each site) with similar levels of metal accumulation were selected to conduct the following RNA-sequencing. Total RNA of each sample was isolated by RNeasy® Mini Kit (QIAGEN) after grinding to powders in liquid nitrogen. The Agilent 2100 was applied to determine the RNA concentration and the RNA integrity number (RIN). All RNAs were eligible for the construction of cDNA library (RIN > 8.0, total RNA > 2 μg).

The genomic DNA was digested by DNase and the mRNA was enriched by Oligo (dT) treatment. These samples were subsequently used to construct the complementary DNA (cDNA) library. More than 20 million reads per sample were obtained from the HiSeq platform (Illumina), with 150-bp paired-end (PE), which were used for bioinformatic analysis (Table 1). Quantitative real-time polymerase chain reaction (qRT-PCR) was used to verify the reliability of high-throughput sequencing. Primers used in qRT-PCR were designed by Primer designing tool on NCBI (Ye et al., 2012), with the temperature for annealing around 60 °C and the fragment length amplified between 100 and 200 bp. All the reagents for qRT-PCR were obtained from the Takara company, including PrimeScript™ RT reagent Kit (Perfect Real Time) and TB Green™ Premix Ex Taq™ II (Tli RNaseH Plus). The conditions for qRT-PCR were 1 cycle, 94 °C for 2 min; 45 cycles, 94 °C for 15 s, 60 °C for 10 s, and 72 °C for 15 s, performed in LightCycler 480 II (Roche). The expression level of gene was calculated by $2^{-\Delta Ct}$ method, with EF-1α (Elongation factor 1α) as the internal reference. The sequences of primers used in qRT-PCR are shown in the Supplementary file 1.

Table 1
Sequence data information.

Number of trimmed reads	S1_rep1	27,482,701
	S1_rep2	25,492,147
	S1_rep3	23,051,485
	S1_rep4	25,649,968
	S1_rep5	26,176,479
	S2_rep1	28,260,103
	S2_rep2	26,051,162
	S2_rep3	23,206,494
	S2_rep4	20,672,120
	S2_rep5	25,588,757
	S3_rep1	21,470,318
	S3_rep2	23,741,921
	S3_rep3	22,751,971
	S3_rep4	23,398,183
	S3_rep5	25,009,725
	In total	368,003,534
Assembly	Number of unigenes	44,801
	Total obtained bases	83,672,011
	Average length	1867
	N50	2619
	L50	10,382
	GC%	39.08%
Assessment the completeness against 978 sequences	Single-copy (S)	843 (86.2%)
	Duplicated (D)	114 (11.7%)
	Fragmented (F)	9 (0.9%)
	Missing (M)	12 (1.2%)
Annotation (e-value ≤1e−5)	Nr	20,342
	Nt	20,101
	Interpro	15,805
	Swiss-Prot	13,846
	KOG	12,335
	KEGG	15,198
	GO	17,729
	In total	27,879

2.4. Bioinformatic analysis

The adaptors and low-quality reads (e.g., N more than 5% and the quality value less than 20) were filtered via trimmomatic software, obtaining the clean reads (Bolger et al., 2014). Then, default parameters except for min_kmer_cov: 3 in Trinity was applied to conduct the *de novo* assembly (Grabherr et al., 2011). Corset software (Davidson and Oshlack, 2014) was applied to reduce the redundancy of assembled transcripts from Trinity, unigenes obtained. The expression of gene was calculated via RNA-Seq by Expectation Maximization (RSEM) after clean reads mapped to assembled unigenes using BOWTIE2 (Langmead and Salzberg, 2012; Li and Dewey, 2011). To receive more convinced results, only

effective unigenes (effective reads mapped in at least 10 samples) were conducted in the following analysis, which was achieved via python scripts (Supplementary file 2). The quality of non-redundant transcripts by Trinity was assessed by BUSCO software against metazoa_odb9 database (Waterhouse et al., 2018). This database containing 978 conserved sequences was downloaded from OrthoDB V9, which is a comprehensive catalog of ortholog and available from https://www.orthodb.org/v9/index.html (Zdobnov et al., 2017). The normalized expression of filtered unigenes based on Transcripts Per Million (TPM) in 15 samples were selected to undergo principal component analysis with the 'ggplot2' package in R with the default parameters (prcomp function with scale as True) (Wickham, 2016). Differentially expressed genes (DEGs, $|\log_2\text{fold-change}| \geq 1$, p-adj < 0.05) were determined with the help of R package edgeR with the raw read counts (Robinson et al., 2009), using the samples in Site 1 as the control. Several public databases, including Non-redundant protein database (Nr), Non-redundant nucleotide databases (Nt), Swiss-Port, and Clusters of orthologous groups of proteins (COG), were employed to predict the function of genes based on the similarity of sequences (e-value <1e−5) by BLAST software (Camacho et al., 2009). Gene Ontology (GO) annotation of genes was predicted by the results of annotation against Nr and Swiss-Prot based on idmapping.tab file downed from public database (ftp://ftp.pir.georgetown.edu/databases/idmapping/idmaping.tb.gz), via python script (Supplementary file 2). For Kyoto Encyclopedia of Genes and Genomes annotation, KEGG Automatic Annotation Server (KASS) was employed to receive the mapped ortholog and pathway (Moriya et al., 2007). On the basis of the hypergeometric test, the functional enrichment of GO and KEGG were analyzed using GOseq software (Young et al., 2010).

3. Results and discussion

3.1. Phenotypic differentiation and metal accumulation

Oysters with similar growth stage (about 2 years, 8–10 cm shell length) were chosen in this study. These oysters exhibited phenotypic variations from different environments. The S1 oysters grew in a relatively uncontaminated environment, whereas oysters from S2 and S3 in metal-rich estuaries were easily distinguished from the normal ones (Fig. 1). The blue-color was only observed in S3 oysters, which was slightly different from the blue-color oysters found in previous studies (Tan et al., 2015; Wang et al., 2011).

Generally, metal concentrations in the gills were the highest among different organs in the oysters. In addition to the difference in tissue color, the accumulation of metals was different among the three sites (Table 2). In general, the concentrations of metals in S1 oysters were relatively low, especially for Cr (2.8 μg/g), Cu (448.0 μg/g), Ni (2.1 μg/g), Pb (0.5 μg/g), and Zn (715.3 μg/g), which were the lowest among the three populations. The lowest Ag and Cd concentrations were found in oysters from Site 2, i.e., 0.4 μg/g and 6.0 μg/g, respectively. Even though no blue color was found in S2, the oysters accumulated 1,600 μg/g Cu and 12,525 μg/g Zn in the gills. In S3, the oysters displayed blue color and contained extraordinarily high levels of metals except for Pb (1.4 μg/g). The Zn and Cu concentrations in S3 oysters were up to 54,955 μg/g (5.5% of tissue body weight) and 3,674 μg/g, which were about 76 times and 7 times higher than those recorded in S1 oysters, respectively.

Table 2
Concentrations of metals (μg /g dry weight.) in the gills of oysters sampled from the three stations. Data are presented as mean ± standard deviation (n = 12). *: Significantly different from S1 (Sig. < 0.05); **: Significantly different from S1 (Sig. < 0.01). S1: Site 1 (Guangxi Province, relatively pristine site), S2: Site 2 (Jiulong River Estuary in Fujian Province, unhealthy oysters sampled), S3: Site 3 (Rong River Estuary in Guangdong Province, blue-colored oysters occurred).

Site/Metal	S1	S2	S3
Ag	1.2 ± 0.5	0.4 ± 0.4**	2.3 ± 1.5*
Cd	22.2 ± 5.3	6.0 ± 0.8**	52.4 ± 5.7**
Cr	2.8 ± 0.7	4.0 ± 0.8*	2.9 ± 1.0
Cu	448.0 ± 261.8	1,601 ± 736**	3,674 ± 1,171**
Ni	2.1 ± 0.9	18.3 ± 2.1**	29.6 ± 3.8**
Pb	0.5 ± 0.1	2.3 ± 0.3**	1.4 ± 0.2**
Zn	715.3 ± 194.4	12,526 ± 5329**	54,955 ± 32,566**

In comparison to the national mapping of oysters documented in the Chinese coastal environment (Lu et al., 2017), concentrations of Ag, Cr, Cu, Ni, Pb and Zn in the oysters from Site 1 were at the background levels, thus Site 1 was regarded as the control and a relatively uncontaminated site. Nearly all the seven metals measured in this study showed significant differences in one-to-one comparison among the three populations except for Cr between S3 and S1 (One-way ANOVA, Sig. < 0.05, SPSS 22.0). With the different levels of metal body burden, oysters from three sites showed distinctive appearance, especially for the blue-colored oyster in S3. Like the previous studies (Luo et al., 2014; Tan et al., 2015; Wang et al., 2011), blue-colored oysters in S3 contained ultra-high trace metal concentrations, especially for Cu (3,674 ± 1,171 μg/g) and Zn (54,955 ± 32,566 μg/g). Therefore, Cu and Zn were the focus of this study, but other metals such as Cd were also considered in the data analysis.

3.2. Transcripts assembly, annotation, and differential expression analysis

A total of 44,801 unigenes were obtained from more than 360 million trimmed-reads from the 15 paired-end sequence samples, via Trinity assembly, Corset clustering and expression filtering (effective reads mapped in at least 10 samples), with an average length of 1,867 bp and an N50 size of 2,619 bp (Table 1). All the raw sequencing data generated by HiSeq™ platform (Illumina) were deposited at the NCBI (Accession No. PRJNA551720). Only 21 sequences in metazoa_odb9 database (978 conserved sequences) were hit as Fragmented (0.9%) and Missing (1.2%) orthologs, suggesting the good completeness of *de novo* assembly (Table 1). 27,879 genes (~62%) of unigenes were matched to at least one public database (Table 1). Principal component analysis (PCA) was conducted to investigate the difference among groups based on the transcriptional profiles (Fig. 2A) (Wickham, 2016). Fifteen samples were discriminated as three clusters clearly and all the 5 biological replicates from each group were clustered together, which indicated the differentiation of gene expression patterns among the three oyster populations and the good reproducibility within a single population. In addition, the different expression profiles (Fig. 2B) were revealed by the pattern of differentially expressed genes (DEGs, $|\log_2\text{fold-change}| \geq 1$, p-adj < 0.05). Due to the lowest metal body burden and the normal morphology, S1 oysters were regarded as the control. Compared to Site 1, 1,342 and 2,460 genes were expressed differentially in Site 2 and Site 3, respectively. Among these DEGs, 603 genes (18.8% in 3199 DEGs) were differentially expressed in both Site 2 and Site 3. Furthermore, 11 genes (EF-1α as internal reference gene and 10 target genes) were selected to conduct qRT-PCR (correlation with the result of RNA-seq, $R^2 > 0.9$), which indicated the reliability of RNA-seq Supplementary file 1).

3.3. Functional enrichment by KEGG and GO

The differentiation under metal stress was revealed by the functional enrichment of DEGs based on the GO and KEGG annotation. A total of 76 and 14 GO terms were enriched significantly in the DEGs (over-represented-FDR < 0.05) in Site 2 and Site 3, respectively

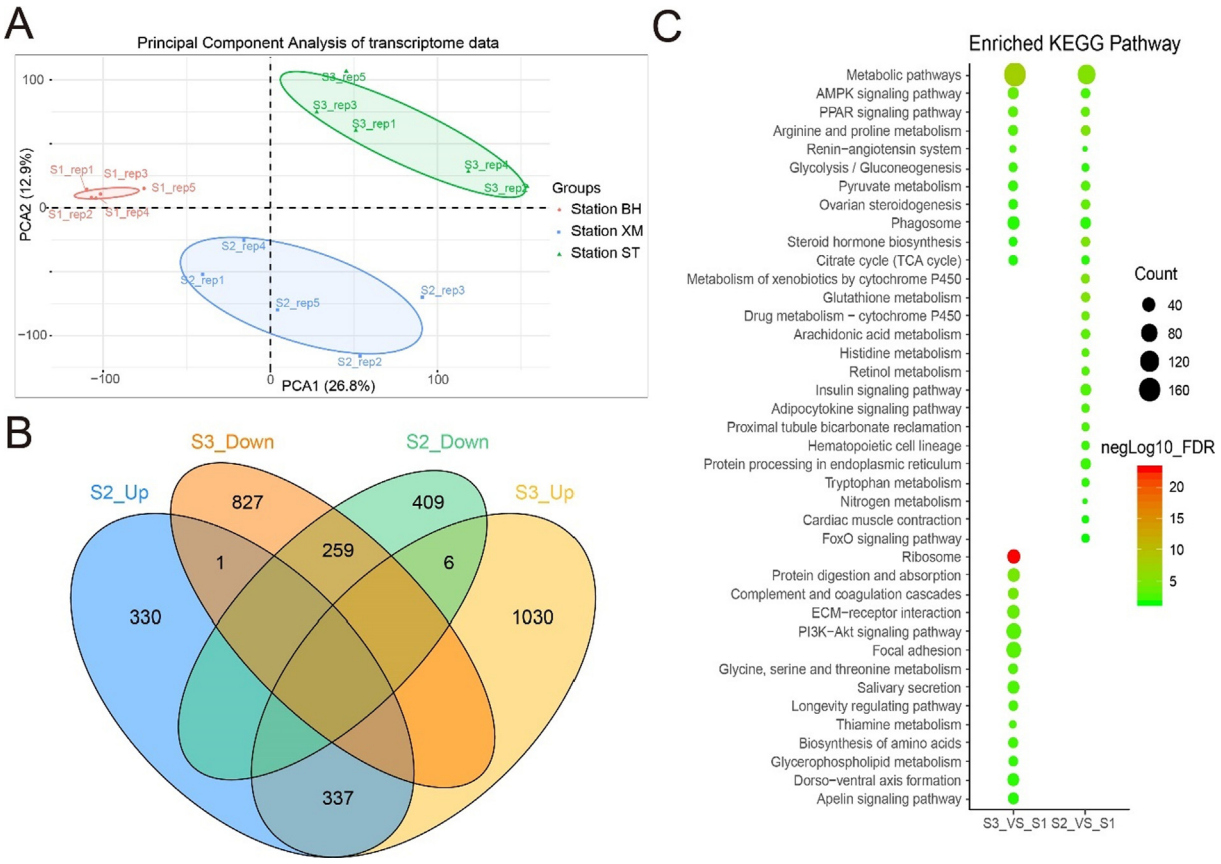

Fig. 2. Differentiation of oysters *C. hongkongensis* at the transcriptional level. A: Principle component analysis of genes expression. B: Transcriptome Venn diagram of DEGs sets from Site 3 (S3), and Site 2 (S2) compared to Site 1 (S1) C: Enrichment of KEGG pathway information. R package ggplot2 was applied to draw the figure (Wickham, 2016).

(Fig. 3, Supplementary files 3 and 4). As for the number of KEGG enrichment, there was no difference in the two contaminated sites, with 26 pathways in Site 2 and 25 pathways in Site 3, respectively. Compared to 11 pathways enriched in both sample sites (Fig. 2C, Supplementary files 5 and 6), there were only 3 GO terms which were significantly enriched in Site 2 and Site 3, which illustrated the differentiation for oysters growing under metal stress at the molecular level (Supplementary files 3 and 4).

Metabolic pathway (ko00010) was highlighted in the two populations containing higher Cu and Zn levels, and was one of the most enriched pathways (Fig. 2C). There were some pathways for the metabolism of molecules enriched, including amino acids, arachidonic acid, retinol, glycerophospholipid, and glutamine. Besides, energy production might be one of the influences derived from metal stress (see Section 3.4.2) and the majority of their constitutes were up-regulated based on the RNA-seq results.

In S3 oysters accumulating up to 5.5% Zn and 0.4% Cu, the constituents of the cytoskeleton and extracellular matrix were targeted (see Section 3.4.3), as shown by the pathway enrichment analysis (Fig. 2C). Furthermore, lower activity of genes participating in the two pathways was detected, and 23 of 25 transcripts in ECM-receptor interaction and 36 of 56 ones in Focal adhesion were down-regulated (Supplementary file 6). In GO level, 9 in 14 terms enriched were related to ribosomal structure and the most enriched pathway was Ribosome, indicating the effect on translation process (Fig. 2C and 3B).

In S2 oysters which accumulated fewer metals (mainly Zn and Cu) than S3 oysters, more GO terms and similar number of pathways were enriched. There were some specificities in oysters from Site 2, including the lower expression of glutathione S-transferase and cytochrome P450 in pathways (drug metabolism – cytochrome P450 and metabolism of xenobiotics by cytochrome P450). The ko04141: protein processing in endoplasmic reticulum was only highlighted in Site 2, with 17 down-regulated transcripts in 19 ones involved.

3.4. Modification of metabolic processes

3.4.1. Enhancement of ion transport and metabolism

Some trace metals are essential for the biochemical reactions as an indispensable element for metalloenzymes, such as Cu and Zn (Harris, 1992). The transportation and regulation of ionic concentration depended on the specific ion channels or transporter proteins or endocytosis (Tessier and Turner, 1995; Wang and Rainbow, 2005). Compared to the S1 oysters, much higher levels of metals were found in the other two sites, especially in Site 3 (up to 5.5% Zn and 0.4% Cu of dry weight, Table 2 and Fig. 4A, B). Such high metal bioaccumulation should directly result from transmembrane transportation.

In this study, one of the key questions was why the oysters were able to accumulate trace metals at high levels, especially for Cu and Zn. Although there was no GO term or pathway related to metal ion transportation and metabolism highlighted via enrichment analysis under the threshold (FDR < 0.05), many genes with these functions were expressed differentially in oysters accumulating higher levels of metals (Site 2 and Site 3).

Besides a large portion of transporters for the macroelements such as sodium and calcium, 3 transcripts responsible for the transportation and metabolism of trace metals (Zn, Cu) were highlighted. Ctr1, the high affinity Cu uptake protein 1, is characterized to play a key role in maintaining the homeostasis of Cu in mammalian cell and yeast, which is responsible for uptake process

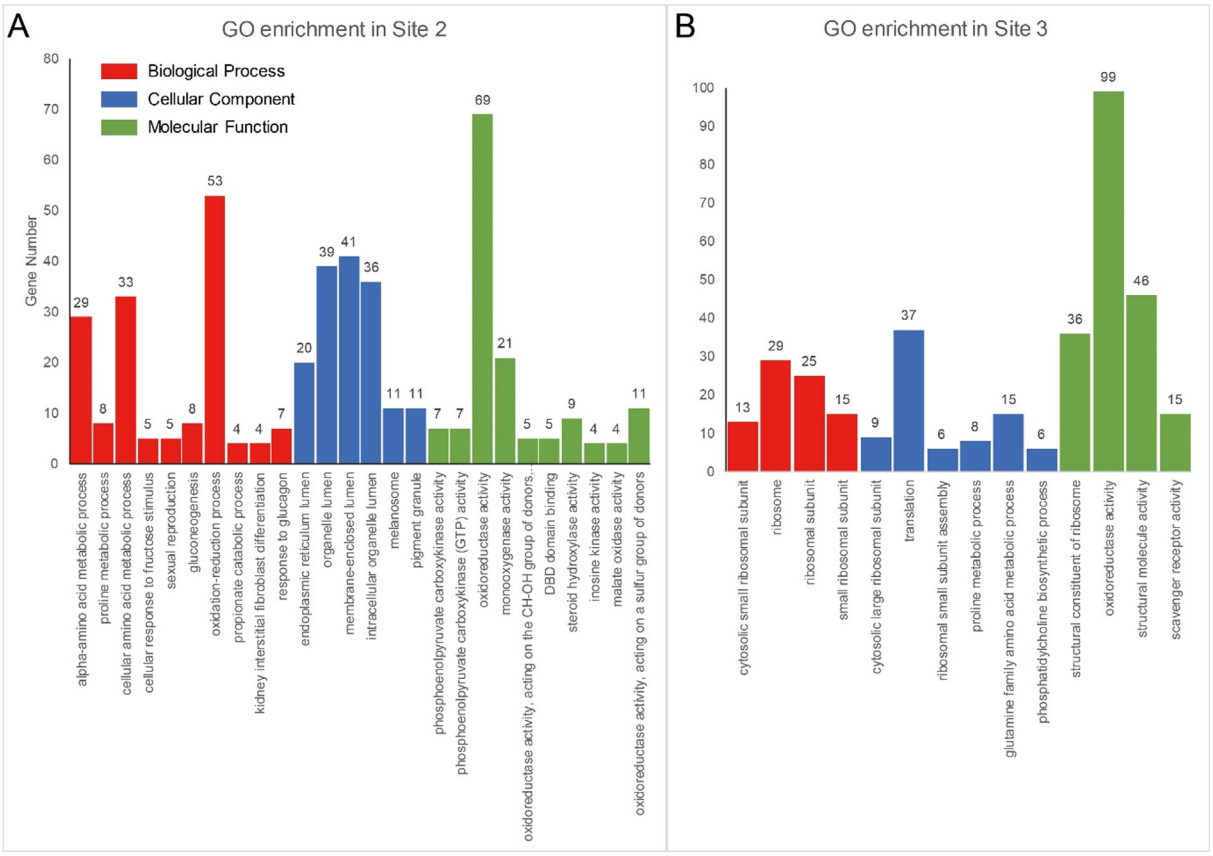

Fig. 3. Enrichment of Gene Ontology. A: GO enrichment in Site 2 (only the most enriched GO terms in three sub-categories are shown). B: GO enrichment in Site 3. The full-list of enrichment results is given in Supplementary files 2 and 3.

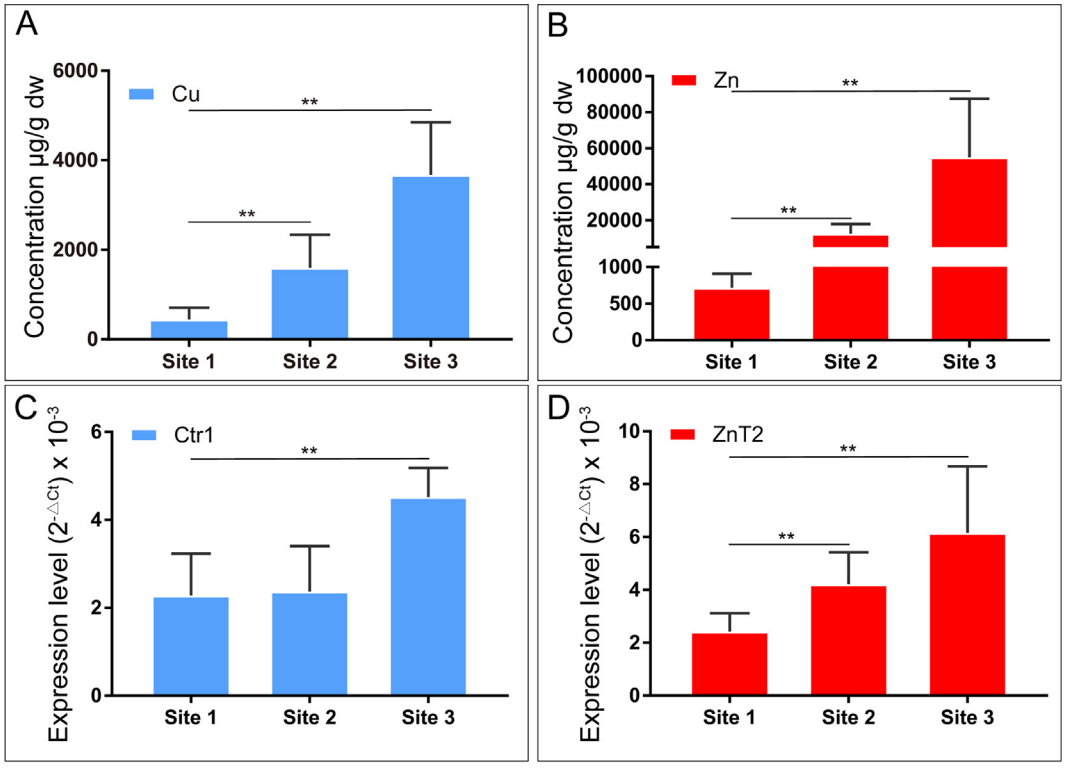

Fig. 4. Metal accumulation and expression of transporters by qRT-PCR. A and B: Cu and Zn accumulation in oysters from three sites. C and D: Ctr1 (high affinity copper uptake protein 1) and ZnT2 (Zinc transporter 2) expression level based on qRT-PCR ($2^{-\Delta Ct}$ method, EF-1α as internal reference). **: Significantly different from S1 (Sig. < 0.01) in one-way ANOVA analysis. Data are shown as Mean ± SD (N = 12).

(Clifford et al., 2016; Kuo et al., 2001). Kuo et al. (2001) reported that Ctr1 is the main avenue of Cu accumulation during the early development of mouse. Also, COPT1 (the homologous of Ctr1 of human) in *Arabidopsis thaliana* was expressed in a high level in root and embryos, and mediated the Cu uptake (Sancenón et al., 2004). Even though such gene is already annotated in *C. gigas* via genome information, there was no study investigating its function under metal contamination. The higher expression level of Ctr1 was only detected in the colored oysters (Site 3), which was 4.05 times in RNA-seq result and about 2 times in qRT-PCR as compared to oysters in Site 1 (Table 3 and Fig. 4C). Up to 4000 μg/g Cu was detected in the gills of colored oysters from Site 3, which might be attributed to the elevated Ctr1 expression.

Two major groups pertaining to Zn solute carrier family (SLC) were already identified in *C. gigas*, including the zinc importer (ZIPs, solute carrier 39A family) for the uptake and the zinc transporters (ZnTs, solute carrier 30 family) for the efflux. In the present study, two transcripts encoding ZnT2 (zinc transporter 2) and ZnT9 (zinc transporter 9) were observed as highly expressed genes in the metal-rich oysters (S2 and S3 oysters) compared to S1 oysters. ZnT2 was expressed at higher levels in oysters with increasing Zn concentration, which was 1.91 times in Site 2 (not significant) and 3.38 times in Site 3 than those in Site 1, respectively (Table 3). Furthermore, the expression change was also observed in qRT-PCR, with a positive trend between Zn accumulation and ZnT2 expression (Fig. 4B and D). The expressions of ZnT9 were significantly higher in oysters with higher metal burden, e.g., 6.03 times in Site 2 and 10.8 times in Site 3 compared to that in Site 1. Unlike ZIPs localized in the cell membrane, proteins encoded by ZnTs (ZnT2 and ZnT9) mainly distributed in the membrane of organelles within the cytoplasm and then participate in Zn transportation from cytoplasm to intracellular compartment or exclude Zn ions, and were highly expressed in the Zn-demanded cells or tissues (Lopez and Kelleher, 2009). The misfunction of ZnT2 in the mammary glands directly down-regulated the ability of Zn export, resulting in the low concentration in milks (Chowanadisai et al., 2006). ZnTs were also verified to regulate the Zn homeostasis in leukocytes in human. Most of the studies on ZnTs focused on the mammals and the function of ZnTs in the Zn hyperaccumulating organisms is unknown. Overexpression of ZnTs in *C. hongkongensis* could lower the bioavailable ions in the cytoplasm via mobilizing Zn ions to vesicles or developing Zn-rich granules, thus contributing the detoxification (Fig. 5). Several genes were not in annotated status due to the unavailable genome information. It was likely that more transporters responsible for Cu and Zn were highly expressed to account for the hyper-accumulation of these two metals, but more molecular experiments are needed to tease out their functions.

In addition to Cu and Zn, other 4 metals (Cd, Ni, Pb, and Ag) were also accumulated differentially among the three sites. There is no evidence to show that Ni is transported via specific proteins although it is essential for many organisms including oysters. The other three metals are non-essential elements, implying that there should not be specific transporters in the organisms. These elements could be imported into the body via other transporters such as calcium channel, Zn transporters, and ATP-binding cassette transporters (ABC transporters). Our RNA-seq results identified some ion transporters (Cu and Zn) with differential expressions, which might also be involved in the accumulation of these metals in oysters. There were similar gradient increases between Ni concentrations and the expression of genes (ZnT9, ZnT2, and Ctr1). For the other three metals, no gene was found with positive correlation with accumulation. During long-term exposure, these metals might be co-imported and co-transported via other identified transporters due to the similar atomic structures as Cu and Zn.

Table 3
Fold changes of genes expression involved in key functions. Only the most significant GENE ID of the same annotated transcript is shown (more details are shown in Supplementary file 7). A: gluconeogenesis. B: glucose import. C: ion transport and metabolism. D: cytoskeleton. E: extracellular matrix. All the transcripts (44,801) assembled are presented in Supplementary file 8, with TPM value, fold-change, and annotation information.

Category	Gene_Name	Transcript_id	S3_VS_S1	S2_VS_S1
A	PEPCK	CL4280.Contig3_All	2.82	14.38
	FBP1	Unigene19261_All	2.60	1.90
B	CREBL2	CL213.Contig2_All	4.60	2.33
C	Zinc transporter 9	CL5450.Contig2_All	10.80	6.03
	Zinc transporter 2	CL11760.Contig2_All	3.38	1.91
	High affinity copper uptake protein 1	CL5412.Contig3_All	4.06	2.01
	MT-IV	CL9855.Contig1_All	53.37	5.51
	Calmodulin	Unigene14385_All	6.05	2.82
D	Gelsolin-like protein	CL11531.Contig1_All	2.45	1.89
	Myosin heavy chain	Unigene12003_All	2.08	2.62
	Tektin-1	CL2198.Contig2_All	2.45	1.16
	Tektin-2	CL8215.Contig1_All	2.28	1.32
	Tektin-3	CL2479.Contig1_All	2.54	1.42
	Tektin-4	Unigene13703_All	2.36	1.23
	Filamin-A	CL4067.Contig2_All	0.23	0.46
	coronin	CL854.Contig2_All	0.49	1.07
	Titin	CL2062.Contig2_All	0.45	0.63
E	Anosmin-1	Unigene19264_All	0.12	0.22
	Laminin subunit gamma-1	CL1601.Contig1_All	0.13	0.26
	Fibrillin-1	CL10369.Contig1_All	0.46	1.05
	collagen alpha chain-like	CL6373.Contig2_All	0.24	0.61
	collagen alpha chain-like	CL3462.Contig1_All	0.35	0.62
	collagen alpha-1(II) chain-like	Unigene15594_All	0.04	0.19
		CL6230.Contig1_All	0.37	0.61
	collagen alpha-1(III) chain-like	Unigene18766_All	0.12	0.56
	Collagen alpha-1(XII) chain	CL1018.Contig2_All	0.09	0.56
	collagen alpha-1(IV) chain-like	CL3944.Contig1_All	0.47	0.98
	collagen alpha-1(IV) chain-like	Unigene2645_All	0.06	0.35
	collagen alpha-3(VI) chain-like	CL878.Contig2_All	0.33	0.79
	short-chain collagen C4-like	Unigene19450_All	0.08	2.21
	short-chain collagen C4-like	CL10683.Contig1_All	10.22	3.42

PEPCK: phosphoenolpyruvate carboxykinase, FBP1: fructose-1,6-bisphosphatase 1. CREBL2: cAMP-responsive element-binding protein-like 2.

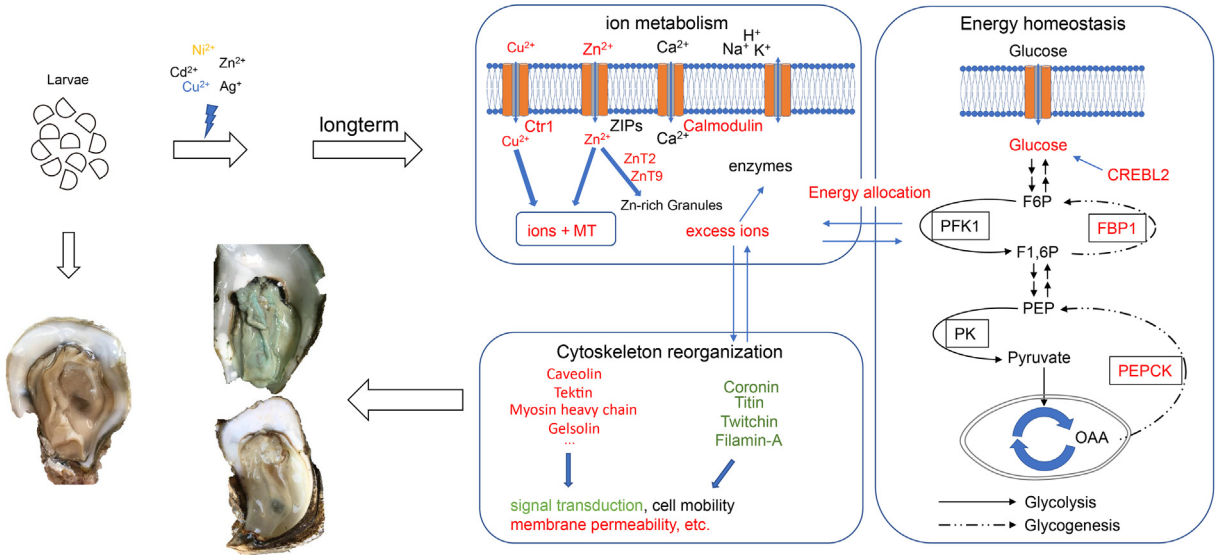

Fig. 5. A possible explanation of trace metal influence on oyster *Crassostrea hongkongensis*. Red color means up-regulation and green color means down-regulation. Ctr1: High affinity copper uptake protein 1. ZnT2: Zinc transporter 2. ZnT9: Zinc transporter 9. Calmodulin: Calmodulin-like protein. MT: Metallothionein IV. CREBL2: cAMP-responsive element-binding protein-like 2. PFK1: 6-phosphofructokinase. F6P: Fructose 6-phosphate. F1,6P: Fructose 1,6-biphosphate. OAA: Oxaloacetate. PEP: Phosphoenolpyruvate. PEPCK: Phosphoenolpyruvate carboxykinase [GTP]. PK: Pyruvate kinase. FBP1: Fructose-1,6-bisphosphatase 1. (For interpretation of the references to color in this figure legend, the reader is referred to the web version of this article.)

Although Cu and Zn are the key elements of many biological enzymes in oysters, over accumulation of these metals would elicit toxicity. Metallothioneins (MTs) are effective molecules in both vertebrates and invertebrates in binding with free metal ions, thus functioning in metal homeostasis and detoxification/storage (Wang and Rainbow, 2010). The cysteine-rich structure of MT allows it to lower the amount of available metal ions within cells. Two transcripts annotated as metallothionein IV (MT-IV) were expressed at low levels in oysters from the pristine environment, with only about 100 TPM value. However, they were identified as DEGs with high expression levels in the contaminated oysters, especially in Site 3 (up to 53.3-fold), followed by a 5.51-fold increase in oysters from Site 2 (Table 3). Oysters (Site 3) with the highest metals (Zn, Cu, and Ni) were detected with the highest metallothionein IV expression. Meanwhile, the second highest metallothionein IV expression was found in oysters from Site 2, containing fewer metals than S3 oysters but higher than S1 oysters. Among these 7 metals measured in this study, the concentrations of Zn and Cu were dozens of times higher than the other metals, and these oysters were found to express more metallothionein IV, which indicated the significant role of metallothionein IV in oysters surviving at such high-levels of metal body burden. It would be necessary to examine the relationships between the amount of free or available ions in oysters and the expression of different levels of metallothionein.

The protein structure of MT (LlMT) of snail *Littorina littorea* revealed the high affinity with divalent metal ions (Cd^{2+}, Zn^{2+}, and Cu^{2+}) (Baumann et al., 2017). Among three metals, the expression of recombinant LlMT in *E. coli* showed the highest level of stimulation in Cd-enriched media by electrospray ionization mass spectrometry (ESI-MS) measurement. Some studies also demonstrated that MT concentration was positively associated with Cd in the oysters *C. hongkongensis* in laboratory exposure experiment (Xu et al., 2015). Cd is regarded to induce the over-expression of MT, with a typically positive correlation between Cd concentration and MT level. In the present study, the lowest level of metallothionein IV expression was not found in S2 oysters with the lowest Cd concentration but in S1 oyster which accumulated the lowest Cu, Zn, and Ni. Similar result was found in a field study of *C. hongkongensis* from metal-contaminated estuary using proteomics technique (Luo et al., 2014). Three metals (Ni, Cu, and Zn) displayed a positive trend with metallothionein IV expression levels in the three populations, but the possibility of Cd inducing MT expression could not be ruled out. Indeed, the presence of Cd may stimulate the increase of MTs, and they could bind together more tightly with each other than MTs with other ions. In realistic environments where Cu and Zn were the dominant metals accumulated in the oysters, these metal ions would be more likely to bind with MTs. The potential influences of Cd may be overwhelmed by Cu or Zn.

3.4.2. Regulation of energy homeostasis

Under stressful environments, energy homeostasis including energy allocation in detoxification and repairment would be impaired due to the excess ions. The genes change suggested that some functions such as the metabolic processes may have been altered under high metal body burden. Among hundreds of DEGs between the contaminated and control oysters, GO terms and KEGG pathways associated with energy homeostasis were significantly enriched in both Site 2 and Site 3 (Supplementary files 3–6). Among the 11 pathways enriched in both sites, some of them participate in metabolic process or energy production including Metabolic pathways, AMPK signaling pathway, PPAR signaling pathway, Glycolysis/Gluconeogenesis, Pyruvate metabolism, and Citrate cycle (TCA cycle), which indicated the important role of energy demand in response to metals stress. Besides the shared pathways, other pathway linked to energy production was also enriched in Site 2, including Insulin signaling pathway (Fig. 2C). Specifically, GO:0004611 (phosphoenolpyruvate carboxykinase activity) was the most significant one in Site 2, which was the key element in gluconeogenesis (Fig. 2A).

For transcripts assigned to the above GO terms and KEGG pathways (Supplementary files 3–6), phosphoenolpyruvate carboxykinase (PEPCK) and fructose-1,6-bisphosphatase 1 (FBP1) in gluconeogenesis were highly expressed in oysters from both contaminated sites. PEPCK is the key enzyme of gluconeogenesis (Fig. 5), catalyzing the first limited step of glucose synthesis from small metabolites (Bacca et al., 2005). According to the annotated results of Nr database, 3 transcripts via *de novo* assembly were

annotated as genes in *C. gigas* genome and were assigned to the same unit in KEGG pathway of *C. gigas* (phosphoenolpyruvate carboxykinase [GTP]). Higher expression of PEPCK were observed in oysters with high metal body burden compared to the less contaminated oysters, up to 28.3-fold change in Site 2 and 5.58-fold change in Site 3. Functioning like PEPCK, FBP1 also played a key role in gluconeogenesis, a rate-limiting enzyme, with a change of 2.60-fold in the most contaminated oysters (Site 3) and higher (but insignificant) expression in Site 2 (Fig. 5, Table 3).

The up-regulation of genes involved in gluconeogenesis might help to increase the balance of glucose and maintain the energy demand for organisms under metal stress (Fig. 5). The high activity of PEPCK likely explained the increased glycogen content in *C. gigas* (Li et al., 2017a). Similar expression patterns of these two genes (FBP1 and PEPCK) were observed in the pearl oyster *Pinctada fucata*, with the higher level of expression in low-temperature resistance species compared to base population (Wang et al., 2018a,b). When faced with pesticide exposure, oyster *C. gigas* also elevated the expression level of FBP1 in proteomic research (Epelboin et al., 2015). The higher energy metabolism would be an adaptation for organisms in response to stresses.

Apart from the higher activity of genes participating in gluconeogenesis, the expression of cAMP-responsive element-binding protein-like 2 (CREBL2) involving in positive regulation of glucose import (GO:0046326, not enriched significantly) also increased in oysters from the contaminated estuaries (Supplementary file 4). The cAMP responsive element binding protein (CREB) family was found as an activator of downstream glucose transporter in human cell line (Chen et al., 2017). There was no study on its role in bivalves, but the function of CREBL2 may be similar to that in mammals, activating the uptake of glucose. In previous studies, the glycogen content was negatively correlated with the levels of trace metal contamination as revealed by the nuclear magnetic resonance (NMR) technique and biomarker measurements (Cao and Wang, 2016, 2017a,b; Liu and Wang, 2016a). Coupled with higher activity of gluconeogenesis, the upregulation of glucose import would result in a higher concentration of glucose, which would be a strategy to cope with energy deficiency under metal contamination.

More energy allocated in some specific aspects would lead to the shortage of others with the change of physical performance (energy trade-off, Bayne, 2004). For example, reduced reproductive activity and the time-lag in oysters (*Ostrea lurida*) were found in the faster growing population (Silliman et al., 2018). External factors could also interfere the energy production and energy allocation in oysters (Dineshram et al., 2013; Li et al., 2017b), such as temperature change (e.g., higher temperature or global warming), salinity, metals, microplastics, and ocean acidification (Cao and Wang, 2017b; Gardon et al., 2018). As the main type of energy reserve, glycogen could reflect the status of individuals. Liu and Wang (2016b) conducted a field experiment by transplanting the oyster *C. hongkongensis* to a contaminated estuary and demonstrated a significant decrease of glycogen content within the first few days of exposure.

In our study, gene regulation of energy metabolism was similar in oysters from the two metal-contaminated sites. By mediating the energy production and allocation, oysters may be able to handle severe metals stress. Oysters *C. hongkongensis* suffering from severe multi-metal stress showed the adaptation potential, e.g., a decrease of uptake whereas a higher capacity for detoxification and elimination (Pan and Wang, 2012a).

3.4.3. Reorganization of cytoskeleton and extracellular matrix

Cytoskeleton not only helps to maintain the normal formation and cell migration, but also plays a key role in signal transduction (Ray and Fry, 2015). Previous studies showed that external stress would reorganize the biological structure of organisms. Under thermal stress, a decreased expression of genes participating in the cytoskeletal structure was observed, including tubulin and myosin (Li et al., 2017b). Although some cytoskeletal genes increased, their down-regulation appeared to be more significant in the hepatopancreas of *C. hongkongensis* from the more contaminated sites (Xu et al., 2016a).

The structural molecules would be one of the target toxicity derived from hyper-accumulated trace metals. Compared to the control Site 1, ECM-receptor interaction (35 transcripts) and Focal adhesion (56 transcripts) were significantly enriched in the oyster from Site 3 (Fig. 2C and Supplementary file 4). The categories based on Gene Ontology clustered the genes responsible to specific functions, although there was not any related term in the result of GO enrichment of Site 3 under the threshold of FDR below 0.05. More than half of the transcripts annotated in extracellular matrix component (GO:0044420) and cytoskeleton categories (GO:0005856) were down-regulated in Site 3, e.g., 82.3% (14 of 17 transcripts) and 58.5% (17 of 29 transcripts), respectively. Less significant results were observed in the less contaminated oysters from Site 2 (less DEGs with no difference between up- and down-regulation in such functional categories).

The expression changes of cytoskeletal genes in contaminated oysters were also more obvious at the highest level of metal contamination. The family of tektin (TEKT I-IV), gelsolin-like protein, microtubule-associated protein, and calmodulin in the contaminated oysters were 2–3 times more expressed when compared to those oysters from the relatively clean environment, with much larger differences observed in oysters from Site 3 (Table 3). The expression of calmodulin increased by 6.05 times compared to the control, indicating that calcium homeostasis was altered possibly under high contaminated Cu and Zn environments. Calmodulin also displayed upregulation in *C. hongkongensis* larvae in response to ocean acidification, which might compensate for the adverse effect of decreased pH (Dineshram et al., 2013, 2015). Similarly, Pb induced an increase of Ca-ATPase expression and disruption of Ca homeostasis (15-fold increase), thus causing severe ER-stress (Meng et al., 2018). On the other hand, compared to Site 1, the expression of remaining cytoskeletal genes in Site 3 oysters declined, and there was only a small difference from Site 2 which was moderately contaminated, such as titin (0.45-fold) and coronin (0.49-fold) (Table 3). Similarly, the expression of Filamin-A was reduced to 0.45 times in Site 2 (without statistic difference) and 0.23 times in Site 3, respectively, as compared to the control site (Table 3). Decreases of cytoskeletal genes or proteins were common in oysters from the stressed environment, meaning that the expression levels of these genes representing the status of cytoskeleton could be used to differentiate whether the organisms were under high metal contamination.

Collagen, an important class of structural protein existing in extracellular space (Mizuta et al., 2004), showed very low expressions in the contaminated oysters. Ten transcripts encoding collagen family were reduced dramatically, although the 5 collagen genes (collagen alpha (type VI) chain) increased in oysters from Site 3 (Table 3). Other extracellular matrix genes similarly showed a decreased expression in Site 3, such as Fibrillin-1 (0.46-fold), Laminin subunit gamma-1 (0.12-fold) and Anosmin-1 (0.11-fold). Decrease of collagen was observed in the Cd-treated mussels *Mytilus galloprovincialis* larvae by proteomic analysis (Xu et al., 2016b). Collagen and other components of ECM were detected in both mantle and shell, indicating their significant roles in shell formation of oyster (Du et al., 2017; Zhang et al., 2012). The expressions of these genes decreased in the contaminated oysters, which may cause a harmful effect on the shell formation, lower strength or formation rate. However, it is difficult to observe the process of shell formation and evaluate the shell strength of oysters.

In this study, uncommon phenotypes were observed in the metal contaminated oysters possibly due to the alteration of

cytoskeleton and ECM. Even though there were some strategies to bind MT and ion-rich granules, the excess ions may cause the production of free radicals or damage of key enzymes involving in protein synthesis. The activity of genes involved in cytoskeleton and ECM were closely linked with other functions, including membrane permeability, signal transduction, apoptosis, and growth (Fig. 5). In our study, several signaling pathways were significantly affected in the contaminated oysters, but the regulation of these indexes remained little known.

4. Conclusion

This study conducted the transcriptome analysis of *C. hongkongensis* chronically exposed to multi-metal contaminations in the field environments. The different metal accumulation was found in these native oyster populations. Cu and Zn were the dominant metals in oysters sampled from the three sites. To our knowledge, this is the first investigation on the molecular mechanisms at the mRNA level in *C. hongkongensis*, a hyper-Cu and Zn accumulation bivalve responding to metal stress. Under different levels of contamination, oysters showed significant differentiation in both gene expression and phenotype (Fig. 5). Disruption of cell structure and enhancement of ion transport were more significant in the oysters containing the highest metals concentrations. The increase of energy budget used in stress was observed in both contaminated sites, which would affect the energy allocation for the normal development. This field sample analysis of oysters provided the gene information under metal exposure in its real status. Besides the toxicity possibly derived from metals, high levels of metals might prompt oysters to regulate the gene expression, thereby resulting in phenotypic variation and differentiation (Fig. 5). However, due to the complexity of the environment, the corresponding effects of single metal could not be identified in this study. Our results mainly focused on the general observation including the gene and apparent differentiation. Furthermore, the relationships between metal accumulation and molecular responses provided or verified some potential biomarkers (e.g., MTs, structural constituents, transporters) responding to complex real-world contaminated environments. Further controlled experiments are needed to have more comprehensive knowledge about the mechanisms employed to accumulate high Cu or Zn concentration and adaptation to stress.

Declaration of Competing Interest

The authors declare that there is no conflict of interest.

Acknowledgement

We thank the anonymous reviewers for their helpful comments on this work. This research was supported by a General Research Fund grant from the Research Grant Council of Hong Kong SAR (16140616).

Appendix A. Supplementary data

Supplementary data to this article can be found online at https://doi.org/10.1016/j.scitotenv.2019.134648.

References

Bacca, H., Huvet, A., Fabioux, C., Daniel, J.Y., Delaporte, M., Pouvreau, S., Van Wormhoudt, A., Moal, J., 2005. Molecular cloning and seasonal expression of oyster glycogen phosphorylase and glycogen synthase genes. Comp. Biochem. Physiol. B: Biochem. Mol. Biol. 140, 635–646.

Bachère, E., Barranger, A., Bruno, R., Rouxel, J., Menard, D., Piquemal, D., Akcha, F., 2017. Parental diuron-exposure alters offspring transcriptome and fitness in Pacific oyster *Crassostrea gigas*. Ecotoxicol. Environ. Saf. 142, 51–58.

Baumann, C., Beil, A., Jurt, S., Niederwanger, M., Palacios, O., Capdevila, M., Atrian, S., Dallinger, R., Zerbe, O., 2017. Structural adaptation of a protein to increased metal stress: NMR structure of a marine snail metallothionein with an additional domain. Angew. Chem. Int. Ed. 56, 4617–4622.

Bayne, B.L., 2004. Phenotypic flexibility and physiological tradeoffs in the feeding and growth of marine bivalve molluscs. Integr. Comp. Biol. 44, 425–432.

Bolger, A.M., Lohse, M., Usadel, B., 2014. Trimmomatic: a flexible trimmer for Illumina sequence data. Bioinformatics 30, 2114–2120.

Camacho, C., Coulouris, G., Avagyan, V., Ma, N., Papadopoulos, J., Bealer, K., Madden, T.L., 2009. BLAST+: architecture and applications. BMC Bioinf. 10, 421.

Cao, C., Wang, W.-X., 2016. Bioaccumulation and metabolomics responses in oysters *Crassostrea hongkongensis* impacted by different levels of metal pollution. Environ. Pollut. 216, 156–165.

Cao, C., Wang, W.-X., 2017a. Chronic effects of copper in oysters *Crassostrea hongkongensis* under different exposure regimes as shown by NMR-based metabolomics. Environ. Toxicol. Chem. 36, 2428–2435.

Cao, C., Wang, W.-X., 2017b. Copper-induced metabolic variation of oysters overwhelmed by salinity effects. Chemosphere 174, 331–341.

Chen, J., Zhang, C., Mi, Y., Chen, F., Du, D., 2017. CREB1 regulates glucose transport of glioma cell line U87 by targeting GLUT1. Mol. Cell. Biochem. 436, 79–86. https://doi.org/10.1007/s11010-017-3080-3.

Chowanadisai, W., Lönnerdal, B., Kelleher, S.L., 2006. Identification of a mutation in SLC30A2 (ZnT-2) in women with low milk zinc concentration that results in transient neonatal zinc deficiency. J. Biol. Chem. 281, 39699–39707.

Clifford, R.J., Maryon, E.B., Kaplan, J.H., 2016. Dynamic internalization and recycling of a metal ion transporter: Cu homeostasis and CTR1, the human Cu^{+} uptake system. J. Cell Sci. 129, 1711.

Cross, I., Merlo, M.A., Rodríguez, M.E., Portela-Bens, S., Rebordinos, L., 2014. Adaptation to abiotic stress in the oyster *Crassostrea angulata* relays on genetic polymorphisms. Fish. Shellfish Immunol. 41, 618–624.

Davidson, N.M., Oshlack, A., 2014. Corset: enabling differential gene expression analysis for de novoassembled transcriptomes. Genome Biol. 15, 410.

Dineshram, R., Quan, Q., Sharma, R., Chandramouli, K., Yalamanchili, H.K., Chu, I., Thiyagarajan, V., 2015. Comparative and quantitative proteomics reveal the adaptive strategies of oyster larvae to ocean acidification. Proteomics 15, 4120–4134.

Dineshram, R., Thiyagarajan, V., Lane, A., Ziniu, Y., Xiao, S., Leung, P.T.Y., 2013. Elevated CO_2 alters larval proteome and its phosphorylation status in the commercial oyster, *Crassostrea hongkongensis*. Mar. Biol. 160, 2189–2205.

Du, X., Fan, G., Jiao, Y., Zhang, H., Guo, X., Huang, R., Zheng, Z., Bian, C., Deng, Y., Wang, Q., Wang, Z., Liang, X., Liang, H., Shi, C., Zhao, X., Sun, F., Hao, R., Bai, J., Liu, J., Chen, W., Liang, J., Liu, W., Xu, Z., Shi, Q., Xu, X., Zhang, G., Liu, X., 2017. The pearl oyster *Pinctada fucata martensii* genome and multi-omic analyses provide insights into biomineralization. GigaScience 6, 1–12.

Epelboin, Y., Quéré, C., Pernet, F., Pichereau, V., Corporeau, C., 2015. Energy and antioxidant responses of pacific oyster exposed to trace levels of pesticides. Chem. Res. Toxicol. 28, 1831–1841.

Gardon, T., Reisser, C., Soyez, C., Quillien, V., Le Moullac, G., 2018. Microplastics affect energy balance and gametogenesis in the pearl oyster *Pinctada margaritifera*. Environ. Sci. Technol. 52, 5277–5286.

Grabherr, M.G., Haas, B.J., Yassour, M., Levin, J.Z., Thompson, D.A., Amit, I., Adiconis, X., Fan, L., Raychowdhury, R., Zeng, Q., Chen, Z., Mauceli, E., Hacohen, N., Gnirke, A., Rhind, N., di Palma, F., Birren, B.W., Nusbaum, C., Lindblad-Toh, K., Friedman, N., Regev, A., 2011. Full-length transcriptome assembly from RNA-Seq data without a reference genome. Nat. Biotechnol. 29, 644.

Gueguen, Y., Denis, S., Adrien, S., Kevin, M., Pierre, G., Solène, B., Marine, N., Patrick, B., Herehia, H., Serge, P., Gilles, L.M., 2017. Response of the pearl oyster *Pinctada margaritifera* to cadmium and chromium: identification of molecular biomarkers. Mar. Pollut. Bull. 118, 420–426.

Harris, E.D., 1992. Copper as a cofactor and regulator of copper, zinc superoxide dismutase. J. Nutr. 122, 636–640.

Heijne, W.H.M., Kienhuis, A.S., van Ommen, B., Stierum, R.H., Groten, J.P., 2005. Systems toxicology: applications of toxicogenomics, transcriptomics, proteomics and metabolomics in toxicology. Exp. Rev. Proteomics 2, 767–780.

Kuo, Y.-M., Zhou, B., Cosco, D., Gitschier, J., 2001. The copper transporter CTR1 provides an essential function in mammalian embryonic development. Proc. Natl. Acad. Sci. U.S.A. 98, 6836.

Lacave, J.M., Vicario-Parés, U., Bilbao, E., Gilliland, D., Mura, F., Dini, L., Cajaraville, M. P., Orbea, A., 2018. Waterborne exposure of adult zebrafish to silver nanoparticles and to ionic silver results in differential silver accumulation and effects at cellular and molecular levels. Sci. Total Environ. 642, 1209–1220.

Langmead, B., Salzberg, S.L., 2012. Fast gapped-read alignment with Bowtie 2. Nat. Methods 9, 357.

Li, B., Song, K., Meng, J., Li, L., Zhang, G., 2017a. Integrated application of transcriptomics and metabolomics provides insights into glycogen content regulation in the Pacific oyster *Crassostrea gigas*. BMC Genomics 18, 713.

Li, B., Dewey, C.N., 2011. RSEM: accurate transcript quantification from RNA-Seq data with or without a reference genome. BMC Bioinf. 12, 323.

Li, J., Zhang, Y., Mao, F., Tong, Y., Liu, Y., Zhang, Y., Yu, Z., 2017b. Characterization and Identification of differentially expressed genes involved in thermal adaptation of the Hong Kong oyster *Crassostrea hongkongensis* by digital gene expression profiling. Front. Mar. Sci. 4, 112.

Liu, F., Rainbow, P.S., Wang, W.-X., 2013. Inter-site differences of zinc susceptibility of the oyster *Crassostrea hongkongensis*. Aquat. Toxicol. 132–133, 26–33.

Liu, S., Guo, C., Lin, W., Wu, F., Lu, G., Lu, J., Dang, Z., 2017. Comparative transcriptomic evidence for Tween80-enhanced biodegradation of phenanthrene by Sphingomonas sp. GY2B. Sci. Total Environ. 609, 1161–1171.
Liu, X., Wang, W.-X., 2016a. Antioxidant and detoxification responses of oysters *Crassostrea hongkongensis* in a multimetal-contaminated estuary. Environ. Toxicol. Chem. 35, 2798–2805.
Liu, X., Wang, W.-X., 2016b. Time changes in biomarker responses in two species of oyster transplanted into a metal contaminated estuary. Sci. Total Environ. 544, 281–290.
Lopez, V., Kelleher, Shannon L., 2009. Zinc transporter-2 (ZnT2) variants are localized to distinct subcellular compartments and functionally transport zinc. Biochem. J. 422, 43.
Lu, G.-Y., Ke, C.-H., Zhu, A., Wang, W.-X., 2017. Oyster-based national mapping of trace metals pollution in the Chinese coastal waters. Environ. Pollut. 224, 658–669.
Luo, L., Ke, C., Guo, X., Shi, B., Huang, M., 2014. Metal accumulation and differentially expressed proteins in gill of oyster (*Crassostrea hongkongensis*) exposed to long-term heavy metal-contaminated estuary. Fish Shellfish Immunol. 38, 318–329.
Meng, J., Wang, W.-X., Li, L., Yin, Q., Zhang, G., 2017a. Cadmium effects on DNA and protein metabolism in oyster (*Crassostrea gigas*) revealed by proteomic analyses. Sci. Rep. 7, 11716.
Meng, J., Wang, W.-X., Li, L., Zhang, G., 2018. Tissue-specific molecular and cellular toxicity of Pb in the oyster (*Crassostrea gigas*): mRNA expression and physiological studies. Aquat. Toxicol. 198, 257–268.
Mizuta, S., Miyagi, T., Nishimiya, T., Yoshinaka, R., 2004. Partial characterization of collagen in several bivalve molluscs. Food Chem. 87, 83–88.
Moriya, Y., Itoh, M., Okuda, S., Yoshizawa, A.C., Kanehisa, M., 2007. KAAS: an automatic genome annotation and pathway reconstruction server. Nucleic Acids Res. 35, W182–W185.
Pan, K., Wang, W.-X., 2012a. Reconstructing the biokinetic processes of oysters to counteract the metal challenges: physiological acclimation. Environ. Sci. Technol. 46, 10765–10771.
Pan, K., Wang, W.-X., 2012b. Trace metal contamination in estuarine and coastal environments in China. Sci. Total Environ. 421–422, 3–16.
Qiao, F., Lei, K., Li, Z., Wei, Z., Liu, Q., Yang, L., He, J., An, L., Qi, H., Cui, S., 2018. Transcriptomic responses of the freshwater snail (*Parafossarulus striatulus*) following dietary exposure to cyanobacteria. Sci. Total Environ. 624, 153–161.
Ray, P.D., Fry, R.C., 2015. Chapter 2 – The Cell: The Fundamental Unit in Systems Biology, Systems Biology in Toxicology and Environmental Health. Academic Press, Boston, pp. 11–42.
Robinson, M.D., McCarthy, D.J., Smyth, G.K., 2009. edgeR: a Bioconductor package for differential expression analysis of digital gene expression data. Bioinformatics 26 (1), 139–140.
Rondon, R., Akcha, F., Alonso, P., Menard, D., Rouxel, J., Montagnani, C., Mitta, G., Cosseau, C., Grunau, C., 2016. Transcriptional changes in *Crassostrea gigas* oyster spat following a parental exposure to the herbicide diuron. Aquat. Toxicol. 175, 47–55.
Sancenón, V., Puig, S., Mateu-Andrés, I., Dorcey, E., Thiele, D.J., Peñarrubia, L., 2004. The *Arabidopsis* copper transporter copt1 functions in root elongation and pollen development. J. Biol. Chem. 279, 15348–15355.
Shi, B., Huang, Z., Xiang, X., Huang, M., Wang, W.X., Ke, C., 2015. Transcriptome analysis of the key role of GAT2 gene in the hyper-accumulation of copper in the oyster *Crassostrea angulata*. Sci. Rep. 5, 17751.
Silliman, K.E., Bowyer, T.K., Roberts, S.B., 2018. Consistent differences in fitness traits across multiple generations of Olympia oysters. Sci. Rep. 8, 6080.
Tan, Q.G., Wang, Y., Wang, W.-X., 2015. Speciation of Cu and Zn in two colored oyster species determined by X-ray absorption spectroscopy. Environ. Sci. Technol. 49, 6919–6925.
Tessier, A., Turner, D.R.D.R., 1995. Metal Speciation and Bioavailability in Aquatic Systems. J. Wiley.
Wang, Q., Liu, Y., Zheng, Z., Deng, Y., Jiao, Y., Du, X., 2018a. Adaptive response of pearl oyster *Pinctada fucata martensii* to low water temperature stress. Fish Shellfish Immunol. 78, 310–315.
Wang, W.-X., Rainbow, P.S., 2010. Significance of metallothioneins in metal accumulation kinetics in marine animals. Comp. Biochem. Physiol. C 152, 1–8.
Wang, W.-X., Rainbow, P.S., 2005. Influence of metal exposure history on trace metal uptake and accumulation by marine invertebrates. Ecotoxicol. Environ. Saf. 61, 145–159.
Wang, W.-X., Meng, J., Weng, N.Y., 2018b. Trace metals in oysters: molecular and cellular mechanisms and ecotoxicological impacts. Environ. Sci. Processes Impacts 20, 892–912.
Wang, W.-X., Yang, Y., Guo, X., He, M., Guo, F., Ke, C., 2011. Copper and zinc contamination in oysters: subcellular distribution and detoxification. Environ. Toxicol. Chem. 30, 1767–1774.
Waterhouse, R.M., Seppey, M., Simão, F.A., Manni, M., Ioannidis, P., Klioutchnikov, G., Kriventseva, E.V., Zdobnov, E.M., 2018. BUSCO applications from quality assessments to gene prediction and phylogenomics. Mol. Biol. Evol. 35, 543–548.
Wickham, H., 2016. ggplot2: Elegant Graphics for Data Analysis. Springer-Verlag, New York. ISBN 978-3-319-24277-4.
Xu, D., Yu, B., Zhang, Y., Cui, M., Zhang, Q., 2015. Metallothionein protein expression of *Crassostrea hongkongensis* in response to cadmium stress. J. Shellfish Res. 34, 311–318.
Xu, L., Ji, C., Wu, H., Tan, Q., Wang, W.-X., 2016a. A comparative proteomic study on the effects of metal pollution in oysters *Crassostrea hongkongensis*. Mar. Pollut. Bull. 112, 436–442.
Xu, L., Peng, X., Yu, D., Ji, C., Zhao, J., Wu, H., 2016b. Proteomic responses reveal the differential effects induced by cadmium in mussels *Mytilus galloprovincialis* at early life stages. Fish Shellfish Immunol. 55, 510–515.
Ye, J., Coulouris, G., Zaretskaya, I., Cutcutache, I., Rozen, S., Madden, T.L., 2012. Primer-BLAST: a tool to design target-specific primers for polymerase chain reaction. BMC Bioinf. 13.
Young, M.D., Wakefield, M.J., Smyth, G.K., Oshlack, A., 2010. Gene ontology analysis for RNA-seq: accounting for selection bias. Genome Biol. 11.
Yu, X.-J., Pan, K., Liu, F., Yan, Y., Wang, W.-X., 2013. Spatial variation and subcellular binding of metals in oysters from a large estuary in China. Mar. Pollut. Bull. 70, 274–280.
Zdobnov, E.M., Tegenfeldt, F., Kuznetsov, D., Waterhouse, R.M., Simão, F.A., Ioannidis, P., Seppey, M., Loetscher, A., Kriventseva, E.V., Ortho, D.B., 2017. v9.1: cataloging evolutionary and functional annotations for animal, fungal, plant, archaeal, bacterial and viral orthologs. Nucleic Acids Res. 45, D744–D749.
Zhang, G., Fang, X., Guo, X., Li, L., Luo, R., Xu, F., Yang, P., Zhang, L., Wang, X., Qi, H., Xiong, Z., Que, H., Xie, Y., Holland, P.W.H., Paps, J., Zhu, Y., Wu, F., Chen, Y., Wang, J., Peng, C., Meng, J., Yang, L., Liu, J., Wen, B., Zhang, N., Huang, Z., Zhu, Q., Feng, Y., Mount, A., Hedgecock, D., Xu, Z., Liu, Y., Domazet-Lošo, T., Du, Y., Sun, X., Zhang, S., Liu, B., Cheng, P., Jiang, X., Li, J., Fan, D., Wang, W., Fu, W., Wang, T., Wang, B., Zhang, J., Peng, Z., Li, Y., Li, N., Wang, J., Chen, M., He, Y., Tan, F., Song, X., Zheng, Q., Huang, R., Yang, H., Du, X., Chen, L., Yang, M., Gaffney, P.M., Wang, S., Luo, L., She, Z., Ming, Y., Huang, W., Zhang, S., Huang, B., Zhang, Y., Qu, T., Ni, P., Miao, G., Wang, J., Wang, Q., Steinberg, C.E.W., Wang, H., Li, N., Qian, L., Zhang, G., Li, Y., Yang, H., Liu, X., Wang, J., Yin, Y., Wang, J., 2012. The oyster genome reveals stress adaptation and complexity of shell formation. Nature 490, 49.
Zhang, Q.-L., Guo, J., Deng, X.-Y., Wang, F., Chen, J.-Y., Lin, L.-B., 2019. Comparative transcriptomic analysis provides insights into the response to the benzo(a) pyrene stress in aquatic firefly (Luciola leii). Sci. Total Environ. 661, 226–234.